

Effective Potential of Higgs Field in Warped Gauge-Higgs Unification

Naoyuki HABA,^{1,*} Shigeki MATSUMOTO,^{2,**} Nobuchika OKADA^{3,***}
and Toshifumi YAMASHITA^{1,4,†}

¹*Department of Physics, Osaka University, Toyonaka 560-0043, Japan*

²*Tohoku University International Advanced Research and Education Organization,
Institute for International Advanced Interdisciplinary Research,
Sendai 980-8578, Japan*

³*Theory Division, KEK, Tsukuba 305-0801, Japan*

⁴*SISSA, Via Beirut 2, I-34014 Trieste, Italy*

(Received May 16, 2008)

Gauge-Higgs unification is one of the influential scenarios for solving the hierarchy problem in the Standard Model. Recently, the scenario on the warped background attracts much attention owing to a large possibility to construct a realistic model naturally in this framework. It is, however, well known that the effective potential for the Higgs field, which is the most important prediction of the scenario, is not easy to calculate on the warped background, because masses of Kaluza-Klein particles are not obtained analytically. In this article, we derive useful formulae for the effective potential. The formulae allow us to calculate Higgs mass easily, and thus to construct a realistic model in the gauge-Higgs unification scenario on the warped background. Using the obtained formulae, we calculate the contributions of bulk fermions with several boundary conditions. We also show that bulk fermions that have boundary conditions prohibited in the orbifold picture do not contribute to the effective potential. The formulae allow us to examine the infrared behavior of the effective potential, and we investigate the Gauge-Higgs condition that the effective theory should satisfy.

§1. Introduction

The Higgs sector is one of the most important sector of the Standard Model (SM), although it is not confirmed yet experimentally. This sector not only governs electroweak symmetry breaking but also gives the masses of quarks and leptons. Furthermore, the hierarchy problem, or to be more precise, the quadratic divergent correction to the Higgs mass strongly suggests the existence of new physics at the TeV scale. This hierarchy problem is expected to be solved at the new physics scale by introducing symmetries. For this purpose, a lot of scenarios beyond the SM have been proposed so far. The most famous example is the supersymmetry (SUSY), in which quadratic divergent corrections to the Higgs mass term are completely cancelled. Another example is the little Higgs scenario, where the corrections are cancelled at the one-loop level owing to an imposed (global) symmetry.

In this article, we discuss the third possibility, the so-called gauge-Higgs (GH)

^{*}) E-mail: haba@het.phys.sci.osaka-u.ac.jp

^{**}) E-mail: smatsu@tuhep.phys.tohoku.ac.jp

^{***}) E-mail: okadan@post.kek.jp

[†]) E-mail: yamasita@het.phys.sci.osaka-u.ac.jp

unification scenario,^{1),2)} in which the Higgs mass term is controlled by higher-dimensional gauge symmetry. In this picture, the Higgs field is identified as the zero mode of the extra-dimensional component of the gauge field. Surprisingly, not only the quadratic divergent corrections but also the other ultraviolet (UV) divergences on the Higgs mass term completely vanish.^{2),3)} Since the imposition of the gauge invariance constrains the model stringently, few constructions of realistic models have been performed, in which the SM correctly appears as the low-energy effective theory of the model. This is in sharp contrast to the case of SUSY or the little Higgs scenario. Recently, a lot of toy models of the GH unification scenario have been considered on flat^{4)–8)} and warped⁹⁾ backgrounds.^{10)–16)} Therefore, we are in the stage of constructing a realistic model in the scenario. Once a realistic model is constructed, it is possible to calculate signals of the models accurately, and test the idea of the GH unification in experiments such as the LHC.

There are two choices for the construction of realistic GH unification models; one is in the flat extra dimension and the other is in the warped extra dimension. The later case seems to be attractive, because essential difficulties in the flat case can be resolved. For example, in the flat case, the typical Kaluza-Klein (KK) scale, Higgs mass and top Yukawa coupling tend to be too small. These problems can be naturally solved in the warped case owing to the volume suppression of the gauge boson mass. Thus, the proper calculation of the effective potential for the Higgs field in the warped background is an important step toward the construction of realistic models.

The effective potential in the warped case, however, has been investigated less exhaustively. This situation is quite different from that in the flat case,^{17)–20)} where even a two-loop calculation has already been performed in a certain model.²¹⁾ The effective potential in the warped case has been evaluated in Ref. 10) for the first time. They evaluated the contribution from a gauge multiplet. A method for the calculation of the potential in a more general setup has been shown in Ref. 12), but it is not easy to use for the construction. In Ref. 22), the method reported in Ref. 10) was generalized in the case in which bulk fermions have parity-odd masses. Recently, more phenomenological analysis has been made in Ref. 23). It was also shown in Ref. 24) that this result can be reproduced by the so-called holographic approach.²⁵⁾

In this article, we review the generalization including antiperiodic fermions, and derive useful approximation formulae for a large warp factor for calculating the effective potential easily. We also examine contributions to the potential from fermions with non-orbifold-like boundary conditions, which are often introduced in warped models.^{12),14),15)} We show that these contributions are vanishing, although such fermions seem to have nonvanishing couplings to the Higgs field. By applying the obtained formulae, we investigate the GH condition²⁶⁾ that the effective theory of the GH unification model should satisfy.

This article is organized as follows. First, in §2, we clarify the setup for deriving formulae for the Higgs effective potential. Next, in §3, we calculate the contribution to the potential of gauge boson loop diagrams. We also explain the method how we can obtain the contribution without knowledge of the KK mass spectrum

concretely. In §4, we derive formulae for contributions from bulk fermions with parity odd masses, and investigate the effective potential using the $SU(3)$ model as an example. In this section, we also examine the effects of the fermion with non-orbifold-like boundary conditions and show that their contributions to the potential are vanishing. Finally, we discuss the GH condition in §5. Section 6 is devoted to summary and discussion.

§2. Setup

In this article, we consider a five-dimensional $SU(2)$ model as a simple example and derive formulae for the Higgs effective potential, unless stated explicitly. The results can be easily applied in more general cases in a way similar to that in Ref. 18). In the model, the $SU(2)$ gauge symmetry is broken down to the $U(1)$ symmetry by the orbifold boundary conditions;²⁷⁾ $A_\mu^{1,2}$ is odd, while A_μ^3 is even. We calculate the effective potential of the zero mode of A_5^2 , setting the vacuum expectation value (VEV) of A_5^1 zero using the residual $U(1)$ symmetry.

The warped metric is taken as⁹⁾

$$ds^2 = G_{MN} dx^M dx^N = e^{-2\sigma(y)} \eta_{\mu\nu} dx^\mu dx^\nu - dy^2, \quad (2.1)$$

where $\sigma(y) = k|y|$ at $-\pi R \leq y \leq \pi R$ and $\sigma(y) = \sigma(y + 2\pi R)$. The four-dimensional flat metric is given by $\eta_{\mu\nu} = \text{diag}(1, -1, -1, -1)$. For clarity, we define $z(y) = e^{\sigma(y)}$, $a = 1/z(\pi R)$ and $\epsilon(y) = \sigma'(y)/k$. As a reference value, we often set the curvature k and the radius R to be $a_0 \equiv \exp(-\pi Rk) = 10^{-15}$.

The action of gauge fields is written as

$$S_g = -\frac{1}{2} \int \sqrt{G} dx^4 dy \text{tr} (F_{MN} F^{MN}) = -\frac{1}{2} \int dx^4 dy \text{tr} (F_{\mu\nu}^2 - 2z^{-2} F_{\mu 5}^2). \quad (2.2)$$

The gauge fixing term is taken to be

$$S_{\text{GF}} = - \int dx^4 dy \text{tr} [D_\mu A_\mu - D_5 (z^{-2} A_5)]^2, \quad (2.3)$$

where $D_{\mu,5}$ is the covariant derivative. Then, we obtain the following equations of motion:

$$(D_\mu^2 - D_5 z^{-2} D_5) A_\nu = 0, \quad z^{-2} (z^2 D_\mu^2 - D_5^2) (z^{-2} A_5) = 0. \quad (2.4)$$

From Eq. (2.4), it turns out that the zero modes of A_5 are proportional to z^2 . Thus, we set the VEV of A_5^2 as

$$g \langle A_5 \rangle = g \langle A_5^2 \rangle \frac{\tau^2}{2} = Az^2 \frac{\tau^2}{2}, \quad (2.5)$$

where τ^2 is the second Pauli matrix. It is worth noting that this zero mode corresponds to the degree of freedom of the Wilson line phase θ_W , as in the flat case, expressed as

$$W \equiv e^{i\theta_W \tau^2} = P \exp \left(-ig \int_{-\pi R}^{\pi R} dy G^{55} A_5 \right) = \exp \left(iA \frac{1-a^2}{2ka^2} \tau^2 \right), \quad (2.6)$$

where P denotes that the integration is the path-ordered one. This leads to the following relation between A and θ_W : $A/k \equiv \widehat{A} = 2a^2\theta_W/(1-a^2)$. In the following discussion, we use hatted parameters as dimensionless parameters in units of the curvature k , e.g., $\widehat{A} = A/k$.

§3. Gauge contribution

In this section, we derive the formula for the Higgs effective potential induced from gauge boson loop diagrams. This contribution has been calculated in Ref. 10). Contributions from fermions are shown in the next section.

3.1. KK mass spectra

Before going to the evaluation of the effective potential, we have to calculate the KK mass spectra of A_μ^1 and A_μ^3 (and also those of A_5^1 and A_5^3). Since we use the convention that only the zero mode of A_5^2 has a nonvanishing VEV, the classical part of the equation of motion in Eq. (2.4) is written as

$$(\partial_\mu^2 - z^{-2}D_5^2 + 2\sigma'D_5) A_\nu = 0, \quad (3.1)$$

where $D_5 = \partial_5 - ig\langle A_5 \rangle$. With new linear combinations, $A_\mu^\pm = (A_\mu^3 \pm iA_\mu^1)/\sqrt{2}$, the covariant derivative D_5 can be represented diagonally as

$$D_5 \begin{pmatrix} A_\mu^+ \\ A_\mu^- \end{pmatrix} = \begin{pmatrix} \partial_5 + iAz^2 & 0 \\ 0 & \partial_5 - iAz^2 \end{pmatrix} \begin{pmatrix} A_\mu^+ \\ A_\mu^- \end{pmatrix}. \quad (3.2)$$

This means that $\chi^\pm \equiv \exp(\mp i \int dy Az^2) A_\mu^\pm$ satisfies the same equation of motion in Eq. (3.1) with the replacement of D_5 by ∂_5 . Then, the equation becomes the usual equation of motion for gauge fields in the case of vanishing VEV. Using this fact, the solutions of the equation can be obtained analytically as,²⁸⁾

$$A_\mu^\pm(x, z) = \sum_{n=0}^{\infty} A_{\mu n}(x) e^{\pm i\epsilon \widehat{A} z^2/2} \frac{e^\sigma}{N_n} [\alpha_n^\pm J_1(\widehat{m}_n z) + \beta_n^\pm Y_1(\widehat{m}_n z)], \quad (3.3)$$

where we have replaced ∂_μ^2 with the KK mass m_n^2 , and assumed $\epsilon^2 = 1$. Here and throughout this article, $J_\nu(x)$ and $Y_\nu(x)$ are the Bessel functions. To obtain the canonical kinetic term for $A_{\mu n}(x)$, the normalization constant N_n appears in the equation. Note that $A_{\mu n}(x)$ is not a complex but a real field, while the coefficients α_n^\pm and β_n^\pm are complex numbers. In the same manner, equations of motion for A_5 fields can be solved as

$$A_5^\pm(x, z) = \sum_{n=0}^{\infty} A_{5n}(x) e^{\pm i\epsilon \widehat{A} z^2/2} \frac{e^{2\sigma}}{N_n} [\alpha_n^\pm J_0(\widehat{m}_n z) + \beta_n^\pm Y_0(\widehat{m}_n z)], \quad (3.4)$$

where $A_5^\pm = (A_5^3 \pm iA_5^1)/\sqrt{2}$.

The KK mass spectra are determined by imposing the boundary conditions at $y = 0$ and $y = \pi R$. We have assumed that A_μ^1 (A_μ^3), which is proportional to $\text{Im}A_\mu^\pm$

$(\text{Re}A_\mu^\pm)$, is odd (even), that is,

$$\left. \frac{d}{dy} \text{Re}A_\mu^\pm \right|_{y=0, \pi R} = 0, \quad \text{Im}A_\mu^\pm \Big|_{y=0, \pi R} = 0. \quad (3.5)$$

Note that the boundary condition for A_μ^- is the same as that for A_μ^+ . Thus, the conditions give four equations for two complex coefficients, $\alpha_n^\pm = (\alpha_n^3 \pm i\alpha_n^1)/\sqrt{2}$ and $\beta_n^\pm = (\beta_n^3 \pm i\beta_n^1)/\sqrt{2}$, which are summarized as

$$\begin{pmatrix} \mathcal{J}_C^{\pi R}(x_n) & -\mathcal{J}_S^{\pi R}(x_n) & \mathcal{Y}_C^{\pi R}(x_n) & -\mathcal{Y}_S^{\pi R}(x_n) \\ \mathcal{J}_C^0(x_n) & -\mathcal{J}_S^0(x_n) & \mathcal{Y}_C^0(x_n) & -\mathcal{Y}_S^0(x_n) \\ s_{\tilde{A}/2} J_1(x_n) & c_{\tilde{A}/2} J_1(x_n) & s_{\tilde{A}/2} Y_1(x_n) & c_{\tilde{A}/2} Y_1(x_n) \\ s_{\hat{A}/2} J_1(ax_n) & c_{\hat{A}/2} J_1(ax_n) & s_{\hat{A}/2} Y_1(ax_n) & c_{\hat{A}/2} Y_1(ax_n) \end{pmatrix} \begin{pmatrix} \alpha_n^3 \\ \alpha_n^1 \\ \beta_n^3 \\ \beta_n^1 \end{pmatrix} = 0, \quad (3.6)$$

where $x_n = m_n/(ka)$, $c_x(s_x) = \cos x(\sin x)$, and $\tilde{A} \equiv A/(ka^2) = 2\theta_W/(1-a^2)$. The functions \mathcal{J} and \mathcal{Y} are given by

$$\begin{pmatrix} \mathcal{J}_C^0(x) \\ \mathcal{J}_S^0(x) \end{pmatrix} = \begin{pmatrix} c_{\tilde{A}a^2/2} & -s_{\tilde{A}a^2/2} \\ s_{\tilde{A}a^2/2} & c_{\tilde{A}a^2/2} \end{pmatrix} \begin{pmatrix} J_1(ax) + axJ_1'(ax) \\ \tilde{A}a^2 J_1(ax) \end{pmatrix}. \quad (3.7)$$

$\mathcal{J}_C^{\pi R}$ and $\mathcal{J}_S^{\pi R}$ are expressed in the same way by replacing a with 1, and \mathcal{Y} is given by these expressions with $J \rightarrow Y$. Nonzero (nontrivial) solutions exist if the determinant of the coefficient matrix, which we denote $M(x_n; \theta_W)$, in Eq. (3.6) vanishes:

$$N(x_n; \theta_W) \equiv \det M(x_n; \theta_W) = 0. \quad (3.8)$$

By solving the equation for the KK mass function $N(x_n; \theta_W)$, the KK mass spectra for the A_μ field is obtained. Also, the KK mass function of the A_5 field is obtained in the same manner, which turns out to be the same as that of A_μ owing to the Higgs-like mechanism. The explicit form of the KK mass function is written as

$$\begin{aligned} N(x; \theta_W) = & -\frac{ax^2}{2} [J_1(x)J_1(ax)Y_0(x)Y_0(ax) + J_1(x)J_0(ax)Y_0(x)Y_1(ax) \\ & + J_0(x)J_1(ax)Y_1(x)Y_0(ax) + J_0(x)J_0(ax)Y_1(x)Y_1(ax) \\ & - 2J_1(x)J_0(x)Y_0(ax)Y_1(ax) - 2J_1(ax)J_0(ax)Y_0(x)Y_1(x)] \\ & + \frac{2}{\pi^2} \cos(2\theta_W). \end{aligned} \quad (3.9)$$

An important property of $N(x; \theta_W)$ is that the function is even with respect to x . This fact plays an essential role in the calculation of the effective potential.

3.2. Effective potential

Once the KK mass function $N(x)$ is obtained, it is possible to calculate the one-loop effective potential

$$V_{\text{eff}} = \sum_i \frac{1}{2} \int \frac{d^4 p}{i(2\pi)^4} \sum_{n=0}^{\infty} \ln(-p^2 + m_n^2), \quad (3.10)$$

where i runs over the indices of the spin and gauge. We have two methods of performing the calculation. The first one is that we carry out the four-momentum integral by the dimensional regularization, then replace the sum of the KK modes with the contour integral, and finally modify the path of the integrals. This method was adopted in Ref. 10) and discussed in detail, for example, in Ref. 29). The second method is that we can take the sum of the KK modes first. For both methods, it is essential that the KK mass function is an even function. In the following, we show the calculation using the second method.

Since the KK mass function is an even function, $m_{-n} \equiv -m_n$ is also a solution in Eq. (3·8). Therefore, the potential in Eq. (3·10) can be written as

$$V_{\text{eff}} = \sum_i \frac{1}{2} \int \frac{d^4 p}{i(2\pi)^4} \frac{1}{2} \sum_{n=-\infty}^{\infty} \ln(-p^2 + m_n^2), \quad (3.11)$$

where n should run also on -0 for taking account of $-m_0$. The summation over n is expressed by the contour integral that encircles the whole real axis counterclockwise. After the Wick rotation, we obtain

$$V_{\text{eff}} = \frac{3}{4} (ka)^4 \int \frac{d^4 l}{(2\pi)^4} \int_C \frac{dx}{2\pi i} \ln(l^2 + x^2) \frac{N'(x; \theta_W)}{N(x; \theta_W)}, \quad (3.12)$$

where l is a dimensionless Euclidean four momentum normalized by ka , and N' denotes dN/dx . Here, we find infinite cuts on the Riemann surface in the partial integration. Since the cut starting from x_n ends at x_{-n} , the surface term vanishes. Thus, the above equation is expressed as

$$V_{\text{eff}} = -\frac{3}{4} (ka)^4 \int_0^\infty \frac{l^3 dl}{8\pi^2} \int_C \frac{dx}{2\pi i} \frac{(l^2 + x^2)'}{l^2 + x^2} \ln[N(x; \theta_W)]. \quad (3.13)$$

Because of the approximation formulae of the Bessel functions at $|x| \rightarrow \infty$,

$$J_\nu(x) \rightarrow \sqrt{\frac{2}{\pi x}} \cos\left(x - \frac{(2\nu + 1)\pi}{4}\right), \quad (3.14)$$

$$Y_\nu(x) \rightarrow \sqrt{\frac{2}{\pi x}} \sin\left(x - \frac{(2\nu + 1)\pi}{4}\right), \quad (3.15)$$

we find the asymptotic behavior of the KK mass function as

$$N(x; \theta_W) \rightarrow -\frac{2}{\pi^2} [\cos\{2(1-a)x\} - \cos(2\theta_W)]. \quad (3.16)$$

This means that, except at $\arg x = 0$, the VEV-dependent part of $\ln[N(x; \theta_W)]$ is exponentially suppressed at $|x| \rightarrow \infty$. Thus, it is possible to modify the contour to that encircling both the upper and lower half planes clockwise, leading to new contours encircling poles at $x = \pm il$. After the contour integral, we obtain

$$V_{\text{eff}}(\theta_W) = \frac{3}{2} \frac{(ka)^4}{(4\pi)^2} \times 2 \int_0^\infty dx x^3 \ln\left[1 + \frac{\cos(2\theta_W)}{N_c(x)}\right], \quad (3.17)$$

where $\bar{N}_c(x)$ is written by the modified Bessel functions $I_\nu(x)$ and $K_\nu(x)$ as

$$\begin{aligned} \bar{N}(x; \theta_W) &\equiv N(ix; \theta_W) \equiv \frac{2}{\pi^2} [\bar{N}_c(x) + \cos(2\theta_W)], \\ \bar{N}_c(x) &= -\frac{2ax^2}{\pi^2} [I_1(x)I_1(ax)K_0(x)K_0(ax) - I_1(x)I_0(ax)K_0(x)K_1(ax) \\ &\quad - I_0(x)I_1(ax)K_1(x)K_0(ax) + I_0(x)I_0(ax)K_1(x)K_1(ax) \\ &\quad + 2I_1(x)I_0(x)K_0(ax)K_1(ax) + 2I_1(ax)I_0(ax)K_0(x)K_1(x)]. \end{aligned} \quad (3.18)$$

The result in Eq. (3.17) is the same as that in Ref. 10) up to a constant term.

§4. Fermion contributions

In this section, we discuss contributions to the effective potential from bulk fermions. The strategy to calculate the contributions is essentially the same as that for the gauge contribution. We consider fermions in the fundamental representation for concreteness. The results obtained in this section can be easily extended to the case of bulk fermions in larger representations.

4.1. Periodic fermion

First, we consider a periodic bulk fermion in the fundamental representation $\Psi = (\Psi_{L,R}^u, \Psi_{L,R}^d)^T$, where Ψ_L^u and Ψ_R^d have zero modes. Since Ψ_R^u (Ψ_L^d) always has the same mass as Ψ_L^d (Ψ_R^u), we consider only Ψ_L and omit the index L in the following discussion. As in the case of the gauge contribution, we calculate the KK mass spectra of the fermion, and evaluate the contribution to the effective potential.

4.1.1. KK mass spectra

As in the case of gauge fields, the wave function of $\Psi^\pm = (\Psi^u \pm i\Psi^d)/\sqrt{2}$ with the kink mass term $-im_\Psi \bar{\Psi}\Psi$ can be obtained analytically as

$$\Psi^\pm(x, z) = \sum_n \Psi_n(x) e^{\pm \frac{i\epsilon Q \hat{A} z^2}{2}} \frac{e^{\sigma/2}}{N_n} [\alpha_n^\pm J_\nu(\hat{m}_n z) + \beta_n^\pm Y_\nu(\hat{m}_n z)], \quad (4.1)$$

where $m_\Psi = c\sigma'$, $\nu = |c + 1/2|$, and $Q = 1/2$. As can be easily understood, the charge dependence of the wave function for bulk fermions in higher representations is given by $\exp[\pm i\epsilon Q \hat{A} z^2/2] \times$ (usual solution), where Q is the eigenvalue of τ^2 .

The boundary conditions for the bulk fermion are given by

$$\left(\frac{d}{dy} \text{Re}\Psi^\pm + c\sigma' \text{Re}\Psi^\pm \right) \Big|_{y=0, \pi R} = 0, \quad \text{Im}\Psi^\pm \Big|_{y=0, \pi R} = 0, \quad (4.2)$$

where the derivative might be replaced by the covariant derivative so that the first condition becomes equivalent to the Dirichlet boundary condition for the corresponding right-handed fermion, $\text{Re}\Psi_R^\pm \Big|_{y=0, \pi R} = 0$, as required by the equation of motion. Note that this modification modifies the coefficient of the lower component of the vector on the right-hand side of Eq. (4.4), which disappears in the determinant (4.5)

and thus does not affect the effective potential. Thus, equations for the coefficients $\alpha_n^{u,d}$ and $\beta_n^{u,d}$ are obtained as

$$\begin{pmatrix} \bar{\mathcal{J}}_C^{\pi R}(x_n) & -\bar{\mathcal{J}}_S^{\pi R}(x_n) & \bar{\mathcal{Y}}_C^{\pi R}(x_n) & -\bar{\mathcal{Y}}_S^{\pi R}(x_n) \\ \bar{\mathcal{J}}_C^0(x_n) & -\bar{\mathcal{J}}_S^0(x_n) & \bar{\mathcal{Y}}_C^0(x_n) & -\bar{\mathcal{Y}}_S^0(x_n) \\ s_{Q\tilde{A}/2}J_\nu(x_n) & c_{Q\tilde{A}/2}J_\nu(x_n) & s_{Q\tilde{A}/2}Y_\nu(x_n) & c_{Q\tilde{A}/2}Y_\nu(x_n) \\ s_{Q\tilde{A}/2}J_\nu(ax_n) & c_{Q\tilde{A}/2}J_\nu(ax_n) & s_{Q\tilde{A}/2}Y_\nu(ax_n) & c_{Q\tilde{A}/2}Y_\nu(ax_n) \end{pmatrix} \begin{pmatrix} \alpha_n^u \\ \alpha_n^d \\ \beta_n^u \\ \beta_n^d \end{pmatrix} = 0, \quad (4.3)$$

where the functions $\bar{\mathcal{J}}$ and $\bar{\mathcal{Y}}$ are given by

$$\begin{pmatrix} \bar{\mathcal{J}}_C^0(x) \\ \bar{\mathcal{J}}_S^0(x) \end{pmatrix} = \begin{pmatrix} c_{Q\tilde{A}a^2/2} & -s_{Q\tilde{A}a^2/2} \\ s_{Q\tilde{A}a^2/2} & c_{Q\tilde{A}a^2/2} \end{pmatrix} \begin{pmatrix} (1/2 + c)J_\nu(ax) + axJ'_\nu(ax) \\ Q\tilde{A}a^2J_\nu(ax) \end{pmatrix}, \quad (4.4)$$

$\bar{\mathcal{J}}_C^{\pi R}$ and $\bar{\mathcal{J}}_S^{\pi R}$ are expressed in the same way by replacing a with 1, and $\bar{\mathcal{Y}}$ is given by these expressions with $J \rightarrow Y$. Note that the case of $c < 0$ can be reproduced from the case of $c > 0$ by the replacement $(\Psi_L^u, \Psi_L^d) \leftrightarrow (\Psi_R^d, \Psi_R^u)$. Thus, we consider the case of $c \geq 0$.

We define the determinant of the coefficient matrix in Eq. (4.3) as $N(x; \theta_W, c, Q)$ as in the previous section. Then, the KK mass spectrum can be found to form zeros of the determinant. After some calculations, the determinant (the KK mass function for the bulk fermion) turns out to be

$$\begin{aligned} N(x; \theta_W, c, Q) &= \frac{2}{\pi^2} [\cos(2Q\theta_W) + N_c(x; c)], \quad (4.5) \\ N_c(x; c) &= 1 + \frac{ax^2\pi^2}{2} [J_{c+1/2}(x)Y_{c-1/2}(ax) - J_{c-1/2}(ax)Y_{c+1/2}(x)] \\ &\quad \times [J_{c-1/2}(x)Y_{c+1/2}(ax) - J_{c+1/2}(ax)Y_{c-1/2}(x)]. \quad (4.6) \end{aligned}$$

It can be seen that the θ_W dependence of $N(x; \theta_W, c, Q)$ comes only from the term $(2/\pi^2) \cos(2Q\theta_W)$. Since the unit of Q is $1/2$, $N(x; \theta_W, c, Q)$ has the shift symmetry $\theta_W \rightarrow \theta_W + 2\pi$, reflecting the phase nature of θ_W . This result is consistent with that obtained in Ref. 13). Below, we discuss the KK mass function $N_c(x; c)$ with some specific values of c , and show an approximate form of the function when $a \ll 1$.

- $c = 0$ case

In the absence of the kink mass term, $c = 0$, $N_c(x; 0)$ has a simple form as

$$N_c(x; 0) = -\cos[2(1-a)x], \quad (4.7)$$

which leads to the KK mass, $m_n = (n\pi \pm \theta_W/2)ka/(1-a)$. Note that the mass spectrum and therefore the effective potential are the same as those in the flat case with the replacement $1/R \leftrightarrow \pi ka/(1-a)$.

- $c = 1/2$ case

When the kink mass is given by $c = 1/2$, $N_c(x; 1/2)$ is

$$\begin{aligned} N_c(x; 1/2) &= 1 + \frac{ax^2\pi^2}{2} [J_0(x)Y_1(ax) - J_1(ax)Y_0(x)] [J_1(x)Y_0(ax) - J_0(ax)Y_1(x)] \\ &\sim 1 + x\pi J_0(x)Y_1(x) - 2x \left[\gamma_E + \ln\left(\frac{ax}{2}\right) \right] J_0(x)J_1(x), \quad (4.8) \end{aligned}$$

where γ_E is Euler's constant. Note that $N_c(x; 1/2)$ is exactly the same as the result of the gauge boson in Eq. (3.9) when $Q = 1$. This coincidence is consistent with the fact that the gaugino field has a kink mass with $c = 1/2$ in a supersymmetric theory with the warped metric.²⁸⁾ The approximation in the last term is valid when $0 < x \ll 1/a$.

- General c case

To obtain a useful approximation of the KK mass function for general c , it is convenient to write the wave function in Eq. (4.1) using J_ν and $J_{-\nu}$ as the basis of the function instead of J_ν and Y_ν . After some calculations, we obtain

$$N_c(x; c) = 1 - \frac{\pi^2 a x^2}{2 \cos^2(c\pi)} \left[J_{1/2+c}(x) J_{1/2-c}(ax) + J_{-1/2+c}(ax) J_{-1/2-c}(x) \right] \\ \times \left[J_{1/2+c}(ax) J_{1/2-c}(x) + J_{-1/2+c}(x) J_{-1/2-c}(ax) \right]. \quad (4.9)$$

As long as we consider a very small a , the contribution of $x > 1/a$ is irrelevant for our calculation. Thus, it is sufficient to know the approximate form valid for $0 < x \ll 1/a$. We expand $J_\nu(ax)$ as

$$J_\nu(x) = \left(\frac{x}{2}\right)^\nu \left[\frac{1}{\Gamma(\nu+1)} - \frac{(x/2)^2}{\Gamma(\nu+2)} + \dots \right]. \quad (4.10)$$

Note that when $-\nu + n < a$, which is realized when $|c| \sim 3/2, 5/2, \dots$, the expansion is inappropriate. However, we are not interested in such a fine-tuned region; we are mainly interested in the case that $|c|$ is not much larger than $1/2$. Then, we find

$$N_c(x, c) = 1 - \frac{\pi x}{\cos(c\pi)} J_{-1/2+c}(x) J_{-1/2-c}(x) \\ + \frac{a^{1-2c} (2c-1) (x/2)^{2-2c} \pi^2 J_{1/2+c}(x) J_{-1/2+c}(x)}{\Gamma^2(3/2-c) \cos^2(c\pi)}, \quad (4.11)$$

for $c > 0$. For $c < 0$, we get the same form with the replacement $c \rightarrow -c$, as it is evident from Eqs. (4.6) and (4.9). Note that the third term on the right-hand side of Eq. (4.11) is exponentially enhanced when $c - 1/2 \gg -1/\ln(a)$ owing to

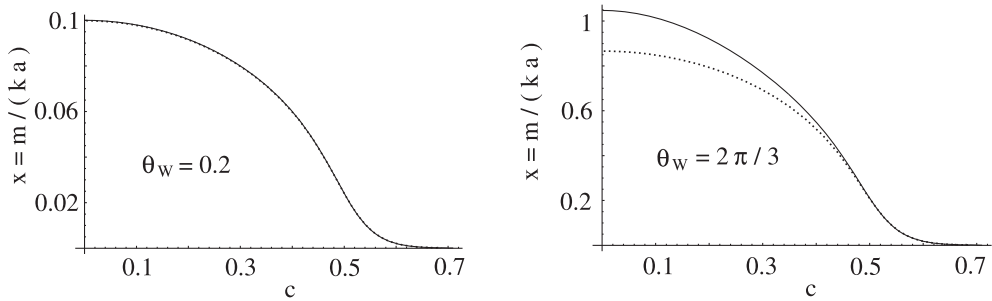


Fig. 1. Mass of first KK mode with $Q = 1/2$ as function of c : The exact result is depicted as a solid line, while the dotted one is the approximation (4.13). We set $\theta_W = 0.2$ and $\theta_W = 2\pi/3$ in the left and right figures, respectively.

the factor a^{1-2c} . In this case, the VEV-independent part is much larger than the VEV-dependent part. This leads to the quite suppressed VEV dependence on the mass spectrum, which is consistent with the fact that the coupling to the Higgs field is suppressed when $|c| > 1/2$.*) When x is small enough, the KK mass function N turns out to be

$$N(x; \theta_W, c, Q) \simeq \frac{\pi^2}{2} \left[\cos(2Q\theta_W) - \frac{1 - 4c^2 - 2(1 - a^{1-2c})x^2}{1 - 4c^2} + \mathcal{O}(x^4) \right], \quad (4.12)$$

which leads to the following formula for the first KK mass:

$$m_1 \sim \sqrt{\frac{(1 - 4c^2)[1 - \cos(2Q\theta_W)]}{2(1 - a^{1-2c})}} ka \rightarrow \sqrt{\frac{[1 - \cos(2Q\theta_W)]}{\ln(a^{-1})}} ka, \quad (4.13)$$

where the limit $c \rightarrow 1/2$ is written. This result is consistent with the approximation formula in Ref. 13). In Fig. 1, we show the validity of the approximation by comparing it with the exact result. As can be seen in the left figure, the approximation formula is quite consistent with the exact one. On the other hand, as shown in the right figure, the approximation becomes worse for a larger $x = m_1/(ka)$ as expected.

We also show the θ_W dependence of the first and second KK masses in Fig. 2 with fixed $c = 0, 0.2, 0.4$ and 0.5 . The figure shows a similar behavior in $c \rightarrow 0$ as in the limit $k \rightarrow 0$ (the flat limit) shown in Ref. 13). Since gauge bosons correspond to $c = 1/2$, the W -boson mass is suppressed compared with the second KK mass. Noting that the gauge boson, or correspondingly the left-handed fermion with $c = 1/2$, has a flat wave function profile along the fifth dimension, we understand that their coupling is generally suppressed by the volume suppression factor $1/\sqrt{\pi R} \propto 1/\sqrt{\ln(a^{-1})}$. On the other hand, fermions with $c = 0$ which are localized around the IR brane around where the Higgs fields are also localized are free of volume suppression. We can see the suppression in fact appears in Eq. (4.13).

4.2. Antiperiodic fermion

Next, we consider bulk fermions obeying antiperiodic boundary conditions. These fermions are used to realize a small Wilson line phase (a small VEV of the Higgs field),⁶⁾ which is required to construct a realistic model consistent with the electroweak precision measurements.¹⁵⁾ Furthermore, the lightest mode of the antiperiodic fermion is stable and a good candidate for dark matter.³⁰⁾

The equation of motion for the fermion on the warped background is the same as that of the periodic fermion, and thus the wave function is also obtained analytically using Bessel functions (4.1). The difference comes only from boundary conditions; the Neumann boundary condition at $y = 0$, while the Dirichlet boundary condition at $y = \pi R$ for Ψ^u ,

$$\left(\frac{d}{dy} \text{Re}\Psi^\pm + c\sigma' \text{Re}\Psi^\pm \right) \Big|_{y=0} = 0, \quad \text{Re}\Psi^\pm \Big|_{y=\pi R} = 0,$$

*) For $|c| > 1/2$, the left-handed fermion localizes around the brane that is the opposite one where the right-handed fermion localizes. Thus, Yukawa coupling is suppressed by small wave function overlapping.

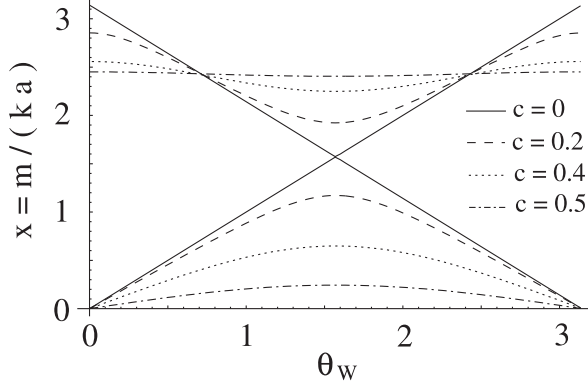


Fig. 2. Masses of first and second KK modes as functions of θ_W : The fermion mass is fixed at $c = 0, 0.2, 0.4$ and 0.5 .

$$\left(\frac{d}{dy} \text{Im} \Psi^\pm + c \sigma' \text{Im} \Psi^\pm \right) \Big|_{y=\pi R} = 0, \quad \text{Im} \Psi^\pm \Big|_{y=0} = 0. \quad (4.14)$$

Note that the opposite boundary conditions, the Dirichlet boundary condition at $y = 0$ and the Neumann boundary condition at $y = \pi R$, give the same result as above, because it can be reproduced by the replacement $\Psi^u \leftrightarrow \Psi^d$. Also, the case of $c < 0$ can be reproduced from the case of $c > 0$ by the replacement, $(\Psi_L^u, \Psi_L^d) \leftrightarrow (\Psi_R^d, \Psi_R^u)$. Thus, we consider the case of $c \geq 0$.

As in the case of the periodic fermion, the KK mass spectrum of the antiperiodic fermion is determined by the zeros of the determinant of the coefficient matrix,

$$M(x) = \begin{pmatrix} \bar{\mathcal{J}}_C^{\pi R}(x) & -\bar{\mathcal{J}}_S^{\pi R}(x) & \bar{\mathcal{Y}}_C^{\pi R}(x) & -\bar{\mathcal{Y}}_S^{\pi R}(x) \\ -c_{Q\hat{A}/2} J_\nu(ax) & s_{Q\hat{A}/2} J_\nu(ax) & -c_{Q\hat{A}/2} Y_\nu(ax) & s_{Q\hat{A}/2} Y_\nu(ax) \\ s_{Q\tilde{A}/2} J_\nu(x) & c_{Q\tilde{A}/2} J_\nu(x) & s_{Q\tilde{A}/2} Y_\nu(x) & c_{Q\tilde{A}/2} Y_\nu(x) \\ \bar{\mathcal{J}}_C^0(x) & \bar{\mathcal{J}}_S^0(x) & \bar{\mathcal{Y}}_C^0(x) & \bar{\mathcal{Y}}_S^0(x) \end{pmatrix}. \quad (4.15)$$

Again, the determinant of the matrix, $N(x; \theta_W, c, Q) = \det M(x)$, depends on the Wilson line phase only through the term $2 \cos(2Q\theta_W)/\pi^2$. Once we define the function $N_c(x; \theta_W)$ as in Eq. (4.5), it becomes independent of θ_W . The function is expressed in a simple form when c is an integer or a half-integer. When c is not a half-integer, we can find its approximation form for $0 < x \ll 1/a$ by expanding the fermion wave function in terms of J_ν and $J_{-\nu}$.

Finally, we find that the N_c of the antiperiodic fermion is given by $-N_c$ of the periodic fermion. This means that the result of the antiperiodic fermion can be obtained from that of the periodic fermion by flipping the sign of $\cos(2Q\theta_W)$, or equivalently by the shift $\theta_W \rightarrow \theta_W + \pi/(2Q)$ as in the flat case.⁶⁾ As a result, the first KK mass of the antiperiodic fermion is approximately given by

$$m_1 \sim \sqrt{\frac{(1 - 4c^2)[1 + \cos(2Q\theta_W)]}{2(1 - a^{1-2c})}} ka, \quad (4.16)$$

when $m_1 \ll ka$.

4.3. Effective potential

Once the KK mass function is explicitly given, the effective potential for the Higgs field is obtained using the method developed in the previous section. Then, the potential is given as

$$V_{\text{eff}}(\theta_W; c, Q) = - \sum_i \frac{1}{2} \frac{(ka)^4}{(4\pi)^2} v_{\text{eff}}(\theta_W; c, Q),$$

$$v_{\text{eff}}(\theta_W; c, Q) = 2 \int_0^\infty dx x^3 \ln \left[1 + \frac{\cos(2Q\theta_W)}{\bar{N}_c(x; c)} \right], \quad (4.17)$$

up to the cosmological constant term. Here, i runs over the indices of the spin, gauge and flavor. The KK mass function on the imaginary axis $\bar{N}_c(x; c)$ is defined as

$$\begin{aligned} \bar{N}_c(x; c) &\equiv N_c(ix; c) \\ &= 1 - \frac{\pi^2 a x^2}{2 \cos^2(c\pi)} \left[I_{1/2+c}(x) I_{1/2-c}(ax) - I_{-1/2+c}(ax) I_{-1/2-c}(x) \right] \\ &\quad \times \left[I_{1/2+c}(ax) I_{1/2-c}(x) - I_{-1/2+c}(x) I_{-1/2-c}(ax) \right], \\ &\sim 1 - \frac{\pi x}{\cos(c\pi)} I_{-1/2+c}(x) I_{-1/2-c}(x) \\ &\quad - \frac{a^{1-2c} (2c-1) (x/2)^{2-2c} \pi^2 I_{1/2+c}(x) I_{-1/2+c}(x)}{\Gamma^2(3/2-c) \cos^2(c\pi)}. \end{aligned} \quad (4.18)$$

In the derivation of the approximation formula, we have used the relation $J_\nu(ix) = i^\nu I_\nu(x)$ and the expansion in Eq. (4.10). In the limit $c \rightarrow 1/2$, the above approximate formula gives

$$\bar{N}_c(x; 1/2) \sim 1 - 2x I_0(x) K_1(x) + 2x \left[\gamma_E + \ln \left(\frac{ax}{2} \right) \right] I_0(x) I_1(x). \quad (4.19)$$

Here, we calculate Higgs mass from the effective potential obtained. To do that, we have to know the relation between A_5 and the four-dimensional Higgs field h . We set $A_5^2 = N^{-1} h z^2$, where N is the normalization factor to have the canonical kinetic term after the integration of the 5th dimension. From the decomposition, we find

$$\mathcal{L}_H = - \int_{-\pi R}^{\pi R} \sqrt{G} dy \frac{1}{2} \text{tr} (F_{MN} F_{PQ}) G^{MN} G^{PQ} \ni \int_{-\pi R}^{\pi R} dy z^2 N^{-2} \frac{1}{2} (\partial_\mu h)^2. \quad (4.20)$$

Therefore, $N = [(1 - a^2)/(ka^2)]^{1/2}$. With the definition of A in Eq. (2.5) and the effective four-dimensional gauge coupling $g_4^2 = g^2/(2\pi R)$, we see $\partial_h^2 = -g_4^2 (1 - a^2) \ln(a)/(2k^2 a^2) \partial_{\theta_W}^2$. Therefore, the Higgs mass is given by

$$m_h^2 = \frac{d^2 V_{\text{eff}}}{dh^2} = -g_4^2 \ln(a) \frac{(ka)^2}{64\pi^2} \sum_i d_i \sum_j \frac{d^2 v_{\text{eff}}}{d\theta_W^2}, \quad (4.21)$$

where $i(j)$ runs over the flavor (gauge) index of each multiplet, and d_i is the number of the spin degree of freedom; for example, $d_i = 3$ for the gauge multiplet and $d_i = -4$

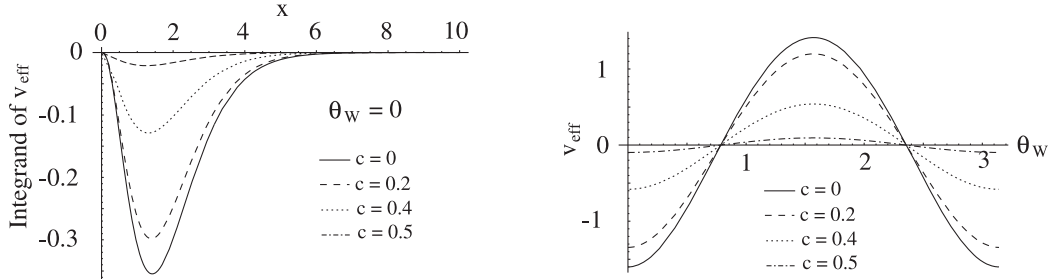


Fig. 3. c dependences of integrand of v_{eff} (left figure) and v_{eff} (right figure): In the left figure, we set $\theta_W = 0$.

for Dirac fermions. Note that the W boson mass is estimated from Eq. (4.13) in the limit $c \rightarrow 1/2$ as $m_W^2 = -(1 - \cos \theta_W)(ka)^2 / \ln a$, which is sufficiently smaller than ka , and thus the approximation is reliable. Then, we obtain

$$m_h^2 = \frac{g_4^2 (\ln a)^2}{64\pi^2 (1 - \cos \theta_W)} m_W^2 \sum_i d_i \sum_j \frac{d^2 v_{\text{eff}}(\theta_W; c_i, Q_a)}{d\theta_W^2}. \quad (4.22)$$

The c dependence of the integrand and that of v_{eff} are shown in Fig. 3. We find that the effective potential is essentially determined by the contribution of region $x \sim 1$; the other regions, $x \ll 1$ and $x \gg 1$, are negligible. Also, we can see that the contribution to the effective potential is smaller for the larger c in the right figure, which is expected from the fact that the Yukawa coupling becomes weaker.

4.4. Model example

In this subsection, we examine the Higgs mass in a concrete model using the formulae derived in this and previous sections. For example, we consider the $SU(3)$ model, where the $SU(3)$ symmetry is broken down to $SU(2) \times U(1)$ by the orbifold breaking. We assume that the components of A_5 corresponding to the $SU(3)/SU(2) \times U(1)$ symmetry have zero modes. We introduce a pair of fundamental fermions with an antiperiodic boundary condition and an adjoint fermion with a periodic one in this model. Their parity odd masses are set to be c_f and c_a , respectively. Then we find that the effective potential of the Higgs field turns out to be¹⁸⁾

$$V_{\text{eff}}(\theta_W) = \frac{(ka)^4}{2(4\pi)^2} \left[3 \left\{ v_{\text{eff}} \left(\theta_W; \frac{1}{2}, 1 \right) + 2v_{\text{eff}} \left(\theta_W; \frac{1}{2}, \frac{1}{2} \right) \right\} - 8v_{\text{eff}} \left(\theta_W + \pi; c_f, \frac{1}{2} \right) - 4 \left\{ v_{\text{eff}}(\theta_W; c_a, 1) + 2v_{\text{eff}} \left(\theta_W; c_a, \frac{1}{2} \right) \right\} \right]. \quad (4.23)$$

Here we fix the mass of the periodic fermion as $c_a = 0.48$. Then, the critical value of c_f to realize $SU(2) \times U(1)$ symmetry breaking becomes $c_f^0 \sim 0.447$. In Fig. 4, the relation between the Higgs mass defined in Eq. (4.22) and θ_W in vacuum is shown by tuning c_f appropriately. We see that the Higgs mass is certainly large compared with m_W , which is in sharp contrast to that in the flat case.

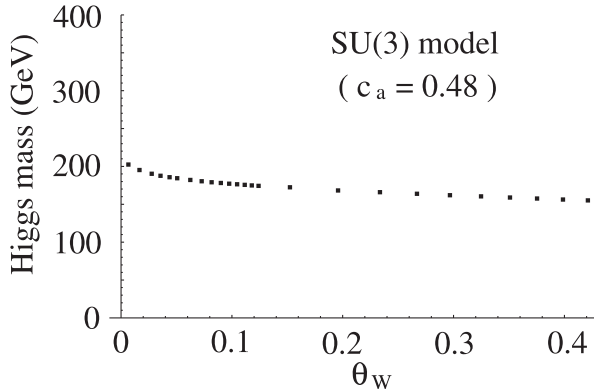


Fig. 4. Relation between Higgs mass and θ_W in vacuum in $SU(3)$ model: Here, we set $m_W = 80$ GeV, $a = a_0 = 10^{-15}$, and $g_4 = 0.6516$.

4.5. Non-orbifold-like fermions

In the $SU(2)$ model, there are four orbifold-like boundary conditions:

$$\begin{pmatrix} N, N \\ D, D \end{pmatrix}, \quad \begin{pmatrix} D, D \\ N, N \end{pmatrix}, \quad \begin{pmatrix} N, D \\ D, N \end{pmatrix}, \quad \begin{pmatrix} D, N \\ N, D \end{pmatrix}, \quad (4.24)$$

where N (D) indicates the Neumann (Dirichlet) condition, the upper (lower) characters show the conditions for Ψ^u (Ψ^d), and the left-side (right-side) characters show the conditions at the boundary on $y = 0$ ($y = \pi R$). Note that these conditions are for Ψ_L , and those for Ψ_R have opposite conditions. Therefore, the first (third) boundary condition becomes the second (fourth) one, if we exchange Ψ^u and Ψ^d . As a result, the second (fourth) condition gives the same contribution as the first (third) one to the effective potential. As can be seen in Eqs. (4.2) and (4.14), the first and third conditions are nothing but those for the periodic and antiperiodic fermions, respectively.

Here, we investigate other possibilities, that is, non-orbifold-like boundary conditions. Such conditions are not consistent with the orbifold picture, but are still allowed if we regard the extra dimension as an interval.³¹⁾ Once we assign the opposite sign for Ψ_R against Ψ_L , there are $2^{2^2} = 16$ possibilities, which comes from two choices, namely, the Neumann or Dirichlet conditions at two boundaries $y = 0$ and πR for two components Ψ^u and Ψ^d . Among them, the above four are orbifold-like, and other four conditions have the same forms as those of four conditions in the remaining eight possibilities by exchanging Ψ^u and Ψ^d . Therefore, there are eight possibilities to examine:

$$\begin{pmatrix} N, N \\ N, N \end{pmatrix}, \begin{pmatrix} N, N \\ N, D \end{pmatrix}, \begin{pmatrix} N, N \\ D, N \end{pmatrix}, \begin{pmatrix} N, D \\ N, D \end{pmatrix}, \begin{pmatrix} D, N \\ D, N \end{pmatrix}, \begin{pmatrix} D, D \\ D, N \end{pmatrix}, \begin{pmatrix} D, D \\ N, D \end{pmatrix}, \begin{pmatrix} D, D \\ D, D \end{pmatrix}. \quad (4.25)$$

These non-orbifold-like boundary conditions can be effectively realized from the orbifold-like ones by introducing boundary-localized (chiral and $SU(2)$ -breaking) fermions with infinitely large mixing masses with bulk fermions.³²⁾ For instance,

let us start from the first option in Eq. (4.24), which implies that the right-handed partner has the second option. Then we introduce boundary fields ψ_R^{u0} and ψ_L^{d0} on $y = 0$ and $\psi_R^{u\pi R}$ and $\psi_L^{d\pi R}$ on $y = \pi R$ to compose localized mixing mass terms:

$$\begin{aligned} & \left(\sqrt{2m_L^0} \psi_R^{u0} \Psi_L^u + \sqrt{2m_R^0} \psi_L^{d0} \Psi_R^d \right) \delta(y) \\ & + \left(\sqrt{2m_L^{\pi R}} \psi_R^{u\pi R} \Psi_L^u + \sqrt{2m_R^{\pi R}} \psi_L^{d\pi R} \Psi_R^d \right) \delta(y - \pi R). \end{aligned} \quad (4.26)$$

When we take the limit $m_R^{0,\pi R} \rightarrow \infty$ (without introducing $\psi_R^{u0,\pi R}$), the wave function of Ψ_R^d vanishes at both boundaries to avoid the large mass terms. This means that the boundary conditions of Ψ_R^d become Dirichlet at both the boundaries, in which the boundary conditions of Ψ_L^d change to the Neumann owing to the equation of motion. Thus, the first boundary condition in Eq. (4.25) is realized. In the same way, other boundary conditions in Eq. (4.25) can be realized from the orbifold-like boundary conditions.

To be more concrete, the above localized mass terms modify the boundary conditions (4.2) as

$$\begin{aligned} \left(\frac{d}{dy} \text{Re}\Psi + c\sigma' \text{Re}\Psi \right) \Big|_{y=0^+, \pi R^-} & \sim -z\gamma^\mu \partial_\mu \text{Re}\Psi_R|_{y=0^+, \pi R^-} \\ & = \mp \frac{z\gamma^\mu \partial_\mu}{2} \sqrt{m_L^{0,\pi R*}} \psi_R^{u0,\pi R}, \end{aligned} \quad (4.27)$$

$$\text{Im}\Psi|_{y=0^+, \pi R^-} = \mp \frac{1}{2} \sqrt{m_R^{0,\pi R*}} \psi_L^{d0,\pi R}, \quad (4.28)$$

where the upper (lower) signs correspond to the boundary conditions at $y = 0$ ($y = \pi R$). Because there are discontinuities of the wave function profiles at the boundaries owing to the mixing masses, we use limits indicated by the superscripts \pm , instead of the values on the boundary for the bulk fermions. Namely, for example, 0^+ denotes $0 + \epsilon$ with a real and positive parameter $\epsilon \rightarrow 0$. In the first line, we use the equation of motion to rewrite the left-hand side by the wave function of the right-handed partner, Ψ_R . Strictly speaking, the derivative should be the covariant one for this purpose. Nevertheless we can do it using the *non-covariant* derivative because the difference does not contribute to the KK mass function calculated below (which is already mentioned above). We can remove the localized fermions in the boundary conditions using their equation of motion,

$$z\gamma^\mu \partial_\mu \psi_L^{0,\pi R} = -\sqrt{m_R^{0,\pi R}} \text{Im}\Psi_R|_{y=0,\pi R}, \quad (4.29)$$

$$z\gamma^\mu \partial_\mu \psi_R^{0,\pi R} = -\sqrt{m_L^{0,\pi R}} \text{Re}\Psi|_{y=0,\pi R}. \quad (4.30)$$

Then, we get

$$zm_n \text{Im}\Psi|_{y=0^+, \pi R^-} = \pm \frac{1}{2} \left| m_R^{0,\pi R} \right| \text{Im}\Psi_R|_{y=0,\pi R}, \quad (4.31)$$

$$zm_n \text{Re}\Psi_R|_{y=0^+, \pi R^-} = \mp \frac{1}{2} \left| m_L^{0,\pi R} \right| \text{Re}\Psi|_{y=0,\pi R}. \quad (4.32)$$

These give four conditions for the four coefficients as before, and we can calculate the KK mass function as

$$\begin{aligned}
N(x) = & \left[(axJ_{c-1/2}(ax) - |\hat{m}_L^0| J_{c+1/2}(ax)) (xJ_{-c+1/2}(x) - |\hat{m}_L^{\pi R}| J_{-c-1/2}(x)) \right. \\
& \left. - (xJ_{c-1/2}(x) + |\hat{m}_L^{\pi R}| J_{c+1/2}(x)) (axJ_{-c+1/2}(ax) + |\hat{m}_L^0| J_{-c-1/2}(ax)) \right] \\
& \times \left[(axJ_{c+1/2}(ax) + |\hat{m}_R^0| J_{c-1/2}(ax)) (xJ_{-c-1/2}(x) + |\hat{m}_R^{\pi R}| J_{-c+1/2}(x)) \right. \\
& \left. - (xJ_{c+1/2}(x) - |\hat{m}_R^{\pi R}| J_{c-1/2}(x)) (axJ_{-c-1/2}(ax) - |\hat{m}_R^0| J_{-c+1/2}(ax)) \right] \\
& - \frac{2 \cos^2(c\pi)}{a\pi^2 x^2} (x^2 + |\hat{m}_L^0| |\hat{m}_R^0|) (a^2 x^2 + |\hat{m}_L^{\pi R}| |\hat{m}_R^{\pi R}|) (\cos(2Q\theta_W) - 1). \quad (4.33)
\end{aligned}$$

This function coincides with Eq. (4.5) in the limit of vanishing all mixing masses up to an overall numerical factor and a factor x^4 , which indicates that there are four additional massless modes. These massless modes correspond to the four boundary fermions which we should remove in the case of vanishing mixing masses. If we introduce one of (m_L^0, m_R^0) while the other is zero, the θ_W -dependent term is suppressed by $1/m_{L,R}^0$ compared with other terms when the mixing masses are sufficiently huge. Thus, the dependence of the KK mass function on θ_W vanishes in the limit $m_{L,R}^0 \rightarrow \infty$. The same discussion can be applied to a pair of $(m_L^{\pi R}, m_R^{\pi R})$. Reminding that m_L (m_R) changes the boundary condition of Ψ^u (Ψ^d), we can see that the dependence remains if and only if the boundary conditions of Ψ^u and Ψ^d are changed at the same time. Interestingly, in such cases, the boundary conditions return to orbifold-like ones. In other words, for fermions with the non-orbifold-like boundary conditions, the KK mass function becomes independent of θ_W , and thus such fermions do not contribute to the effective potential of θ_W .

However, this conclusion seems strange, in a sense. This is because the coupling of the non-orbifold-like fermions to the Higgs field seems nonvanishing. For instance, let us consider the flat limit $k \rightarrow 0$. In this case, the Ψ^u component of the fermion with the first boundary condition in Eq. (4.25) interacts with the Higgs field with Ψ_R^d , which has a (D, D) boundary condition. It is easy to see that the overlap integral among the zero mode of Ψ^u , the lowest mode of Ψ_R^d , $\sin(y/R)$, and the zero mode of A_5 is nonvanishing. The reason the contributions of the non-orbifold-like fermions vanish might be related to the fact that a (N, N) mode (Ψ^u) does not couple to a (D, D) mode (Ψ_R^d) through θ_W in the orbifold picture. However, we do not yet have a clear understanding at this stage, and we leave this as an open question.

Before closing this section, let us comment on Eq. (4.33). In the above discussion, we use only the limits of $m \rightarrow 0$ or $m \rightarrow \infty$ for examining the Neumann and Dirichlet boundary conditions. However, we can take a finite value for the mixing mass, and in fact this is often used in model building in the GH unification scenario to make unwanted zero modes massive. The expression (4.33) can be used for such cases.

§5. Gauge-Higgs condition

In this section, we examine the GH condition in the warped background. The condition has first been proposed in Ref. 26) in the context of the GH unification

scenario in the flat background.

The basic idea of the GH condition comes from the fact that, below the compactification scale, the effective theory should be described by only zero modes in the usual four-dimensional field theory. Since the Higgs field is merely a scalar field in the effective theory, its potential receives divergent corrections and need to be renormalized. The cutoff scale of the effective theory is expected to be around the compactification scale, and the theory is defined by renormalization conditions at the cutoff scale. We call the condition on the Higgs quartic coupling as the GH condition. Once we settle these conditions, we can perform analysis in terms of a familiar four-dimensional framework such as renormalization group equations, which is a powerful tool for investigating low-energy phenomena of the GH unification scenario.

5.1. GH condition in the flat background

Before going to the discussion of the GH condition in a warped background, we briefly review the condition in the flat case. In Ref. 26), we have investigated the effective potential of the Higgs field in the flat five-dimensional space-time. Contributions to the effective potential of the Higgs field from periodic and antiperiodic fermions are analytically written as (up to constant term)

$$\sum_{w=1}^{\infty} \frac{\cos(wx)}{w^5} = \zeta_R(5) - \frac{x^2}{2!} \zeta_R(3) + \frac{x^4}{4!} \frac{1}{2} \left[\frac{25}{6} - \ln(x^2) \right] + \mathcal{O}(x^6), \quad (5.1)$$

$$\sum_{w=1}^{\infty} \frac{\cos[w(x - \pi)]}{w^5} = -\frac{15}{16} \zeta_R(5) + \frac{x^2}{2!} \frac{3}{4} \zeta_R(3) - \frac{x^4}{4!} \ln(2) + \mathcal{O}(x^6), \quad (5.2)$$

with the overall coefficient $C/2 = 3/(4\pi^2(2\pi R)^4)$. Additional minus signs appear for the contribution of bosons.¹⁸⁾ Here, $\zeta_R(x)$ is Riemann's zeta function and $x = Qg_4 2\pi R h = m_1/\Lambda_{UV}$, where Q is the charge, $\Lambda_{UV} = (2\pi R)^{-1}$ is the cutoff scale of the four-dimensional effective theory and m_1 is the mass of the zero mode acquired after symmetry breaking.

In the quadratic term of x^2 , the contributions of antiperiodic modes are of the same order as those from periodic ones, and have opposite signs. Since antiperiodic fermions have no zero modes (the mass of the lightest mode is of the order of the cutoff scale), this fact means that the mass parameter can be treated as a free parameter as long as we are interested in the low-energy effective theory in the GH unification scenario. Unlike those in the quadratic term, contributions come mostly from periodic modes in the quartic term when $x \ll 1$.

On the other hand, the effective potential is also calculated in the framework of the effective theory. The contribution to the quartic term from the zero mode of a periodic fermion with a charge Q turns out to be

$$V_{\text{eff}} \Big|_{h^4} = \frac{1}{4!} \left[\lambda(\mu) + \frac{b}{2} (Qg_4)^4 \left\{ \ln \left(\frac{h^2}{\mu^2} \right) - \frac{25}{6} \right\} \right] h^4, \quad (5.3)$$

where $\lambda(\mu)$ is defined by

$$\lambda(\mu) = \frac{d^4 V_{\text{eff}}}{dh^4} \Big|_{h=\mu}, \quad (5.4)$$

which is the renormalized coupling defined at the scale μ ,³³⁾ and $b = -3/\pi^2$ is the coefficient of the beta function of $\lambda(\mu)$ concerning the Yukawa coupling of the zero mode with the Higgs field. By comparing this result with Eq. (5.1) (the spin degree of freedom is 4), we find the renormalization condition as

$$\lambda\left(\frac{1}{Qg_4L}\right) = \lambda\left(\frac{1}{Qg_42\pi R}\right) = 0. \quad (5.5)$$

This is the GH condition in the five-dimensional model in the flat background. Since usually $Qg_4 = \mathcal{O}(1)$, the running coupling constant vanishes around the cutoff scale Λ_{UV} . Practically, we can also find the cutoff scale Λ_{UV} from the fourth derivative of the effective potential around the origin, which is obtained from Eq. (5.1) as

$$\left.\frac{d^4V_{\text{eff}}}{dh^4}\right|_{h \rightarrow 0} = \frac{b}{2}y^4 \ln\left(\frac{m_1^2}{\Lambda_{UV}^2}\right), \quad (5.6)$$

where $y = Qg_4$ is the Yukawa coupling of the zero mode. Interestingly, this is nothing but the renormalization effect of the coupling from the cutoff scale Λ_{UV} down to the zero mode mass m_1 , neglecting the Yukawa coupling flow.

5.2. GH condition in warped background

The GH condition is consistent with the physical speculation that the Higgs self interaction should vanish above the compactification scale where the five-dimensional gauge invariance will be recovered. Therefore, it is expected that a similar condition also holds in the warped case. In such a case, however, it is not clear which scale is the compactification scale. In fact, the typical scale of the first KK mass $m_{KK} = \pi ka$ is far from the ‘radius’ $1/R$. Unfortunately, it is difficult to investigate the effective potential analytically in the warped case. Instead, we perform numerical analyses to find the cutoff scale Λ_{UV} . Here, we examine the effective potential induced by a periodic mode with a charge $Q = 1/2$,

$$V_{\text{eff}}(\theta_W; c, 1/2) = \frac{1}{2} \frac{(ka)^4}{(4\pi)^2} 2 \int_0^\infty dx x^3 \ln\left(1 + \frac{\cos \theta_W}{N_c(x; c)}\right), \quad (5.7)$$

where we fix the warp factor to $a = a_0 = 10^{-15}$. The contribution of an antiperiodic mode is given simply by $V_{\text{eff}}(\theta_W + \pi; c, 1/2)$.

First, let us see the scale dependence of the running quartic coupling defined in Eq. (5.4). In Fig. 5, we show the fourth derivative of the potential $V_{\text{eff}}^{(4)}(\theta_W) \equiv d^4V_{\text{eff}}(\theta_W; c, 1/2)/d\theta_W^4$ as a function of θ_W . In the left figure, $V_{\text{eff}}^{(4)}(\theta_W)$ is normalized by the prefactor $(ka)^4/(32\pi^2)$. Since

$$\frac{d^4}{dh^4} = \frac{g_4^4(1-a^2)^2(\ln(a))^2}{4(ka)^4} \frac{d^4}{d\theta_W^4}, \quad (5.8)$$

the running coupling in Eq. (5.4) is obtained by multiplying $2(\ln(a_0)/(16\pi))^2 g_4^4 \sim 0.94g_4^4$ to the fourth derivative $V_{\text{eff}}^{(4)}(\theta_W)$. When c close to 0, the coupling is so large that the perturbative calculation is not reliable. The reason we show such unreliable

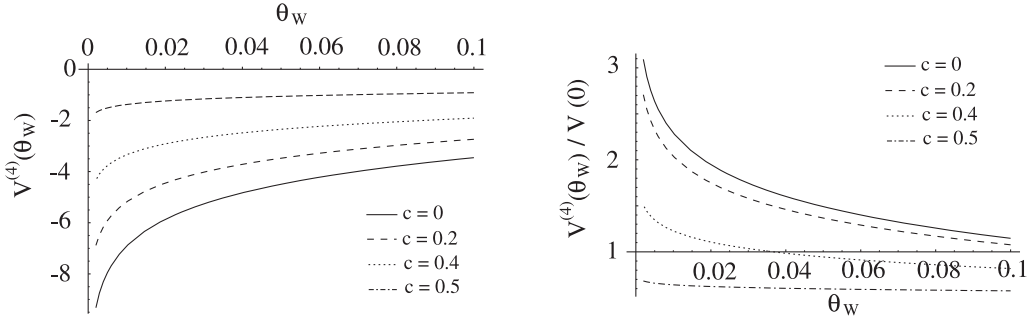


Fig. 5. Scale dependence of running quartic coupling: The fermion mass is fixed at $c = 0, 0.2, 0.4$ and 0.5 , respectively. In the left figure, the fourth derivative of the potential is shown as a function of θ_W , while it is normalized by $V_{\text{eff}}^{(4)}(0; c, 1/2)$ in the right figure.

results is to compare them with reliable ones (with c close to $1/2$). Since the potential in the $c = 0$ case is the same as that in the flat model, the GH condition is given by that in §5.1. Therefore, with the correspondence $1/R \leftrightarrow \pi ka/(1-a)$, the GH condition in Eq. (5.5) holds at $\mu = ka/(2Qg_4(1-a))$ in the $c = 0$ case. The results in Fig. 5 show that the potential with a smaller c has a stronger IR divergence. In other words, the effect of the constant term in $V_{\text{eff}}^{(4)}(\theta_W)$ becomes more relevant for the mode with c closer to $1/2$. Thus, the scale of the GH condition is larger for larger c . This means that there is a nonvanishing threshold effect at $\mu = ka/(2Qg_4(1-a))$, which is the counterpart of the scale in the flat case.

This fact seems to be natural, because, in the warped background, it is well known that the profiles of KK modes tend to approach the IR ($y = \pi R$) brane; thus, the modes have larger Yukawa couplings with the Higgs field (which also localizes around the IR brane) than the zero modes. As a result, the contributions of the KK modes are relatively enhanced, and their effects on quartic coupling are expected to appear as threshold corrections. These threshold corrections from the KK modes at the compactification scale are sizable in the warped GH unification models, in contrast to the flat models.

Next, we discuss contributions to the potential of the antiperiodic modes. The contributions to the quadratic term (mass parameter) are shown in Fig. 6 (left figure) using the second derivative of the potential at $\theta_W = \pi$ as

$$V_{\text{eff}}^{(2)}(\theta_W) \equiv \frac{d^2 V_{\text{eff}}(\theta_W; c, 1/2)}{d\theta_W^2} = -\frac{1}{2} \frac{(ka)^4}{(4\pi)^2} 2 \int_0^\infty dx x^3 \frac{1 + \bar{N}_c(x; c) \cos \theta_W}{(\bar{N}_c(x; c) + \cos \theta_W)^2}, \quad (5.9)$$

normalized by $V_{\text{eff}}^{(2)}(0)$ as a function of c . This ratio is nothing but that between antiperiodic and periodic modes. As can be seen in the figure, the contributions of antiperiodic modes are comparable to those of periodic ones, as in the flat case.

The contributions to the quartic term of antiperiodic modes are shown in Fig. 6, where the ratio $-V_{\text{eff}}^{(4)}(\pi)/V_{\text{eff}}^{(4)}(\theta_W)$ is depicted as a function of c for $\theta_W = 0.1, 0.01$ and 0.001 . Note that the potential with $c = 0$ is the same as that in the flat case.

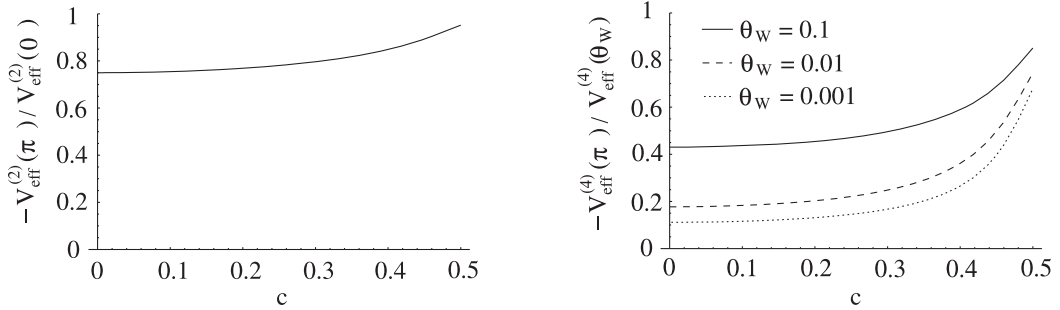


Fig. 6. Contributions to potential of antiperiodic modes: In the left figure, the contribution ratio of antiperiodic to periodic modes is shown. In the right figure, the Wilson phase is set to be $\theta_W = 0.1, 0.01$ and 0.001 .

We see that contributions of antiperiodic modes are suppressed at small θ_W when $c \ll 1$, as expected. On the other hand, for c close to $1/2$, the contributions are comparable to those of the periodic modes. One of the reasons for this should be the fact that the mass of the lightest mode of the antiperiodic fermion is much smaller than the typical KK mass m_{KK} . Also, the result is consistent with the fact that the threshold corrections from the KK modes are more important for larger c . The figure implies that the contribution of the running effect below the first KK mass is not large, which is different from that in the flat case. Unfortunately, it seems difficult to find an analytical expression for threshold corrections from the KK modes.

§6. Summary and discussion

In this article, we have derived formulae for calculating the effective potential of the Higgs field in the gauge-Higgs unification scenario in the Randall-Sundrum background. They can be applied even when we introduce bulk fermions with arbitrary parity-odd bulk mass terms and boundary conditions. These formulae will be useful not only for analyzing the GH unification scenario but also for constructing realistic models having many attractive features.^{11)–15)}

We have also calculated the contributions to the potential of bulk fermions with boundary conditions that are not allowed in the orbifold picture. As a result, we have shown that their contributions vanish even though they seem to couple with the Higgs field. This might be related to the fact that the orbifold parity forbids coupling in the orbifold picture, but we have not found a clear reason why the contributions vanish, and leave this as an open question. Nevertheless, we note that the expression of the KK mass function, which is used to calculate the effective potential, is useful for finite values of mixing masses, although we derived it to examine the contribution of non-orbifold-like fermions in the limit of zero or infinite mixing masses.

Since the formulae allow us to calculate Higgs potential exactly at one-loop level, the potential properly incorporates its infrared behavior. Thus, we have examined the GH condition²⁶⁾ in the warped background. In a flat case, the running coupling of quartic Higgs interaction vanishes at the compactification scale. On the other

hand, in the warped models, we found that the coupling has a substantial value already at the scale of typical KK mass. This fact can be understood as threshold corrections from KK modes, because the interactions of Higgs with KK modes are strong compared with those with zero modes. Although it is not easy to evaluate threshold corrections analytically, once we find a way to evaluate them, it will become possible to investigate GH models on the warped background in the framework of the well-established four-dimensional field theory. We leave this problem for future work.

Acknowledgements

T. Y. would like to thank K. Oda for useful discussions. This work is supported in part by a Grant-in-Aid for Science Research from the Ministry of Education, Culture, Sports, Science and Technology, Japan (Nos. 16540258 and 17740146 for N. H. and No. 18740170 for N. O.). T. Y. is supported in part by The 21st Century COE Program “Towards a New Basic Science; Depth and Synthesis”.

References

- 1) N. S. Manton, Nucl. Phys. B **158** (1979), 141.
D. B. Fairlie, J. of Phys. G **5** (1979), L55; Phys. Lett. B **82** (1979), 97.
- 2) Y. Hosotani, Phys. Lett. B **126** (1983), 309; Ann. of Phys. **190** (1989), 233; Phys. Lett. B **129** (1983), 193; Phys. Rev. D **29** (1984), 731.
- 3) N. V. Krasnikov, Phys. Lett. B **273** (1991), 246.
H. Hatanaka, T. Inami and C. S. Lim, Mod. Phys. Lett. A **13** (1998), 2601.
G. R. Dvali, S. Randjbar-Daemi and R. Tabbash, Phys. Rev. D **65** (2002), 064021.
N. Arkani-Hamed, A. G. Cohen and H. Georgi, Phys. Lett. B **513** (2001), 232.
I. Antoniadis, K. Benakli and M. Quiros, New J. Phys. **3** (2001), 20.
- 4) C. Csaki, C. Grojean and H. Murayama, Phys. Rev. D **67** (2003), 085012.
G. Burdman and Y. Nomura, Nucl. Phys. B **656** (2003), 3.
N. Haba and Y. Shimizu, Phys. Rev. D **67** (2003), 095001 [Errata; **69** (2004), 059902].
I. Gogoladze, Y. Mimura and S. Nandi, Phys. Lett. B **560** (2003), 204; Phys. Lett. B **562** (2003), 307.
K. Choi, K. S. Jeong, K. Okumura, N. Haba, Y. Shimizu and M. Yamaguchi, J. High Energy Phys. **02** (2004), 037.
G. Cacciapaglia, C. Csaki and S. C. Park, J. High Energy Phys. **03** (2006), 099.
- 5) C. A. Scrucca, M. Serone and L. Silvestrini, Nucl. Phys. B **669** (2003), 128.
C. A. Scrucca, M. Serone, L. Silvestrini and A. Wulzer, J. High Energy Phys. **02** (2004), 049.
G. Martinelli, M. Salvatori, C. A. Scrucca and L. Silvestrini, J. High Energy Phys. **10** (2005), 037.
G. Panico, M. Serone and A. Wulzer, Nucl. Phys. B **739** (2006), 186.
- 6) N. Haba, M. Harada, Y. Hosotani and Y. Kawamura, Nucl. Phys. B **657** (2003), 169 [Errata; **669** (2003), 381].
N. Haba, Y. Hosotani, Y. Kawamura and T. Yamashita, Phys. Rev. D **70** (2004), 015010.
N. Haba and T. Yamashita, J. High Energy Phys. **04** (2004), 016.
N. Haba, K. Takenaga and T. Yamashita, Phys. Lett. B **615** (2005), 247.
- 7) Y. Hosotani, S. Noda and K. Takenaga, Phys. Rev. D **69** (2004), 125014; Phys. Lett. B **607** (2005), 276.
- 8) K. Hasegawa, C. S. Lim and N. Maru, Phys. Lett. B **604** (2004), 133.
- 9) L. Randall and R. Sundrum, Phys. Rev. Lett. **83** (1999), 3370.
- 10) K. Oda and A. Weiler, Phys. Lett. B **606** (2005), 408.
- 11) R. Contino, Y. Nomura and A. Pomarol, Nucl. Phys. B **671** (2003), 148.
- 12) K. Agashe, R. Contino and A. Pomarol, Nucl. Phys. B **719** (2005), 165.

- A. D. Medina, N. R. Shah and C. E. M. Wagner, *Phys. Rev. D* **76** (2007), 095010.
- 13) Y. Hosotani and M. Mabe, *Phys. Lett. B* **615** (2005), 257.
Y. Hosotani, S. Noda, Y. Sakamura and S. Shimasaki, *Phys. Rev. D* **73** (2006), 096006.
- 14) Y. Sakamura and Y. Hosotani, *Phys. Lett. B* **645** (2007), 442.
Y. Hosotani and Y. Sakamura, *Prog. Theor. Phys.* **118** (2007), 935.
Y. Sakamura, *Phys. Rev. D* **76** (2007), 065002.
- 15) K. Agashe and R. Contino, *Nucl. Phys. B* **742** (2006), 59.
M. S. Carena, E. Ponton, J. Santiago and C. E. M. Wagner, *Nucl. Phys. B* **759** (2006), 202; *Phys. Rev. D* **76** (2007), 035006.
- 16) G. F. Giudice, C. Grojean, A. Pomarol and R. Rattazzi, *J. High Energy Phys.* **06** (2007), 045.
A. Falkowski, S. Pokorski and J. P. Roberts, *J. High Energy Phys.* **12** (2007), 063.
- 17) M. Kubo, C. S. Lim and H. Yamashita, *Mod. Phys. Lett. A* **17** (2002), 2249.
A. Delgado, A. Pomarol and M. Quiros, *Phys. Rev. D* **60** (1999), 095008.
K. Takenaga, *Phys. Lett. B* **570** (2003), 244.
A. Aranda and J. L. Diaz-Cruz, *Phys. Lett. B* **633** (2006), 591.
- 18) N. Haba and T. Yamashita, *J. High Energy Phys.* **02** (2004), 059.
- 19) C. S. Lim and N. Maru, *Phys. Lett. B* **653** (2007), 320.
Y. Adachi, C. S. Lim and N. Maru, *Phys. Rev. D* **76** (2007), 075009.
C. S. Lim and N. Maru, *Phys. Rev. D* **75** (2007), 115011.
- 20) K. Kojima, K. Takenaga and T. Yamashita, *Phys. Rev. D* **77** (2008) 075004.
- 21) N. Maru and T. Yamashita, *Nucl. Phys. B* **754** (2006), 127.
Y. Hosotani, N. Maru, K. Takenaga and T. Yamashita, *Prog. Theor. Phys.* **118** (2007), 1053.
- 22) A. Falkowski, *Phys. Rev. D* **75** (2007), 025017.
- 23) H. Hatanaka, arXiv:0712.1334.
- 24) G. Panico and A. Wulzer, *J. High Energy Phys.* **05** (2007), 060.
- 25) M. A. Luty, M. Porrati and R. Rattazzi, *J. High Energy Phys.* **09** (2003), 029.
R. Barbieri, A. Pomarol and R. Rattazzi, *Phys. Lett. B* **591** (2004), 141.
- 26) N. Haba, S. Matsumoto, N. Okada and T. Yamashita, *J. High Energy Phys.* **02** (2006), 073.
I. Gogoladze, N. Okada and Q. Shafi, *Phys. Lett. B* **655** (2007), 257.
- 27) Y. Kawamura, *Prog. Theor. Phys.* **103** (2000), 613; *Prog. Theor. Phys.* **105** (2001), 691; *Prog. Theor. Phys.* **105** (2001), 999.
- 28) S. Chang, J. Hisano, H. Nakano, N. Okada and M. Yamaguchi, *Phys. Rev. D* **62** (2000), 084025.
D. Marti and A. Pomarol, *Phys. Rev. D* **64** (2001), 105025.
- 29) W. D. Goldberger and I. Z. Rothstein, *Phys. Lett. B* **491** (2000), 339.
- 30) M. Regis, M. Serone and P. Ullio, *J. High Energy Phys.* **03** (2007), 084.
- 31) C. Csaki, C. Grojean, H. Murayama, L. Pilo and J. Terning, *Phys. Rev. D* **69** (2004), 055006.
- 32) N. Haba, Y. Sakamura and T. Yamashita, *J. High Energy Phys.* **06** (2008), 044.
- 33) S. R. Coleman and E. Weinberg, *Phys. Rev. D* **7** (1973), 1888.